

AD 687439

High-Temperature Mass Spectrometry

Volume I: Free Vaporization Studies of Graphites

Prepared by F. M. WACHI and D. E. GILMARTIN
Materials Sciences Laboratory

69 JAN 27

Laboratory Operations
AEROSPACE CORPORATION

Prepared for SPACE AND MISSILE SYSTEMS ORGANIZATION
AIR FORCE SYSTEMS COMMAND
LOS ANGELES AIR FORCE STATION
Los Angeles, California

DDC
RECEIVED
MAY 26 1969
C

THIS DOCUMENT HAS BEEN APPROVED FOR PUBLIC
RELEASE AND SALE: ITS DISTRIBUTION IS UNLIMITED

Reproduced by the
CLEARINGHOUSE
for Federal Scientific & Technical
Information Springfield Va. 22151

**BLANK PAGES
IN THIS
DOCUMENT
WERE NOT
FILMED**

Air Force Report No.
SAMSO-TR-69-12: VOL. I

Aerospace Report No. ~~2~~
TR-0200(4250-40)-6, Vol I

HIGH-TEMPERATURE MASS SPECTROMETRY
Volume I: Free Vaporization Studies of Graphites

Prepared by
F. M. Wachi and D. E. Gilmartin
Materials Sciences Laboratory

69 JAN 27

Laboratory Operations
AEROSPACE CORPORATION

Prepared for
SPACE AND MISSILE SYSTEMS ORGANIZATION
AIR FORCE SYSTEMS COMMAND
LOS ANGELES AIR FORCE STATION
Los Angeles, California

This document has been approved for public release
and sale; its distribution is unlimited

FOREWORD


This report is published by the Aerospace Corporation, El Segundo, California, under Air Force Contract No. FO 4701-68-C-0200.

This report, which documents research carried out from November 1965 to April 1968, was submitted on 20 March 1969 to Lieutenant Jerry J. Smith, SMTM, for review and approval.

The authors are greatly indebted to R. L. Joyce for preparation of specimens for microstructure determinations, J. H. Richardson for his assistance in the interpretation of the photomicrographs, E. S. Elliot for x-ray diffraction analyses of the various graphites, and Drs. J. E. Colwell and W. T. Barry for their helpful discussions.


Part of this dissertation was presented at the Twenty-First Pacific Coast Regional Meeting of the American Ceramic Society held 23-25 October 1968 in Pasadena, California.

Approved



W. C. Riley, Director
Materials Sciences Laboratory

Publication of this report does not constitute Air Force approval of the report's findings or conclusions. It is published only for the exchange and stimulation of ideas.



Jerry J. Smith
2nd Lt., United States Air Force
Project Officer

ABSTRACT

Some of the differences in the published data on the free vaporization of conventional (ATJ, ZTA, UT-6) and pyrolytic graphites have been resolved. Relative abundances, relative rates of vaporization, and activation energies of vaporization have been measured for carbon species C_1 through C_5 , for conventional graphites in the temperature range $2800^\circ - 3000^\circ K$, and for pyrolytic graphite in the temperature range $2600^\circ - 3260^\circ K$. Differences in the free evaporation behavior of the two types of graphites are discussed. Plausible vaporization mechanisms are presented that account for the time dependency of species distribution at constant surface temperature for conventional graphites, and for the differences in activation energies of vaporization for C_4 and C_5 molecules vaporizing from pyrolytic and conventional graphites. The effects of the differential rates of carbon evaporation from the crystalline and binder phases on the free vaporization behavior of conventional graphites at temperatures greater than about $2950^{+50} K$ are described.

CONTENTS

FOREWORD	11
ABSTRACT	111
I. INTRODUCTION	1
II. EXPERIMENTAL	3
A. Equipment	3
B. General Procedure for Mass Spectrometric Analysis of Carbon Vapor	7
C. Materials	9
III. RESULTS AND DISCUSSION	11
A. Pyrolytic Graphite	11
B. Conventional Graphites	18
IV. CONCLUSIONS	35
REFERENCES	37

FIGURES

1. Cutaway View of Langmuir Cell and Water-Cooled Vacuum Housing	4
2. CEC Model 21-110 Mass Spectrometer and Langmuir Cell, with its Associated Equipment	8
3. Ionization Efficiency Curve for C_3 Molecule from A-Face of Pyrolytic Graphite	12
4. Arrhenius Plots for Carbon Species Vaporizing from C-Face of Pyrolytic Graphite	16
5. Photomicrographs of Cross Section of ZTA Graphite Heated to $2627^{\circ}K$. .	24
6. Arrhenius Plots for Carbon Species Vaporizing from Machined Surfaces of UT-6 Graphite	26
7. Arrhenius Plots for C_2 and C_3 Molecules Vaporizing from Machined Surfaces of ATJ and ZTA Graphites	27
8. Variation of Surface Temperature with Power Input for ATJ and ZTA Graphites	28
9. Arrhenius Plots for Carbon Species Vaporizing from Machined Surfaces of Conventional Graphites After Specimens Were Heated to $2950^{\circ}K$	30

TABLES

1. Physical Properties of Graphites	10
2. Ion Intensity Ratios for Pyrolytic Graphite	14
3. Apparent Activation Energies of Vaporization of Carbon Species for Pyrolytic Graphite	17
4. Ion Intensity Ratios for Conventional Graphites	19
5. Variation in Ion Intensity Ratio with Time at $2627^{\circ}K$ for ZTA Graphite	20
6. Apparent Activation Energies of Vaporization of Carbon Species from Machined Surfaces of Conventional Graphites	32

I. INTRODUCTION

In spite of extensive research carried out over the past two decades, the mechanism of graphite vaporization is still undefined. Quantitative data regarding rates of vaporization and molecular weight distribution of the vapor species have been controversial or entirely lacking at temperatures above 2900°K. For example, JANAF data on vapor pressure, when extrapolated to the triple-point temperature of graphite, yield a triple-point pressure two orders of magnitude lower than the currently accepted value.¹ This disagreement is critical in reentry technology since, during a substantial portion of reentry time, graphitic thermal protection materials are subjected to temperatures and pressures higher than the triple-point temperature and pressure of graphite. Since the calculation of recession rates involves vaporization kinetics and thermochemistry, it is necessary to (1) clarify the differences in existing vaporization data and (2) take advantage of newly developed instrumentation and techniques in order to extend the data to higher temperatures.

Vaporization studies have been conducted, either under essentially equilibrium condition by the Knudsen effusion method² or under free vaporization condition by the Langmuir rate method,³ to obtain both thermodynamic and kinetic data. A summary on graphite vaporization data and a critical evaluation of the differences in existing vaporization data have been made by Palmer and Shelef;¹ interested readers should consult this reference.

We are concerned here only with the free vaporization behavior of graphites. The work described herein resolves some of the differences in the published data on the free vaporization of graphites, and presents new vaporization data for conventional (ATJ, ZTA, UT-6) and pyrolytic graphites. Relative abundances, relative rates of vaporization, and activation energies of vaporization have been measured for carbon species C_1 through C_5 , for conventional graphites in the temperature range 2800° - 3000°K, and for pyrolytic graphite in the temperature range 2600° - 3260°K. Differences

in the free evaporation behavior of the two types of graphites are discussed. Plausible vaporization processes are postulated for the conventional graphites to account for the time dependency of species distribution observed at constant surface temperature under nonequilibrium vaporization condition. The effects of the differential rates of carbon evaporation from the crystalline and binder phases on the free vaporization behavior of conventional graphites at temperatures in excess of 2950°K are described.

II. EXPERIMENTAL

A. EQUIPMENT

At the initiation of our experimentation, we used a time-of-flight mass spectrometer (Bendix Corp., Model 14) modified to accept the Langmuir vaporization cell shown in Fig. 1. The existing Knudsen cell housing was replaced with a vacuum chamber of similar design but with a slightly larger internal diameter in the water-cooled tower section. This vacuum chamber was connected to the ion source chamber by a 7.6×0.76 mm slit, and was evacuated using a pumping station supplied with the spectrometer. After several experiments, it became apparent that this spectrometer was inadequate for use in unequivocal identification of carbon vapor species of mass greater than that of the C_2 molecule because of its inherently low mass resolving power; e.g., this equipment could not resolve the ionic masses from interfering ionic masses resulting from impurities in the graphite specimen and from residual hydrocarbon vapors in the mass spectrometer.

For most of the work reported herein, we used a high-resolution, double-focusing mass spectrometer (Consolidated Electrodynamics Corp., Model 21-110) fitted with an ion source (Model 140527) designed for Knudsen cell studies so that it could also accommodate the Langmuir vaporization cell. The Langmuir cell was coupled to the ion source housing by a water-cooled vacuum chamber equipped with a beam shutter that could be operated from outside the chamber. A cutaway view of the Langmuir vaporization cell and the water-cooled vacuum chamber is shown in Fig. 1. Differential pumping was maintained across the slit separating the two chambers by an auxiliary pumping station (Veeco, Model VS 400). The pumping station was connected to the water-cooled vacuum chamber by a stainless steel pipe 10.2 cm o.d. and 102 cm long. With this two-chamber system, a source pressure of less than 2×10^{-6} Torr was maintained even when the pressure in the Langmuir cell housing reached 8×10^{-6} Torr. The latter pressure was attained only when the graphite specimen was heated to temperatures above 2950°K.

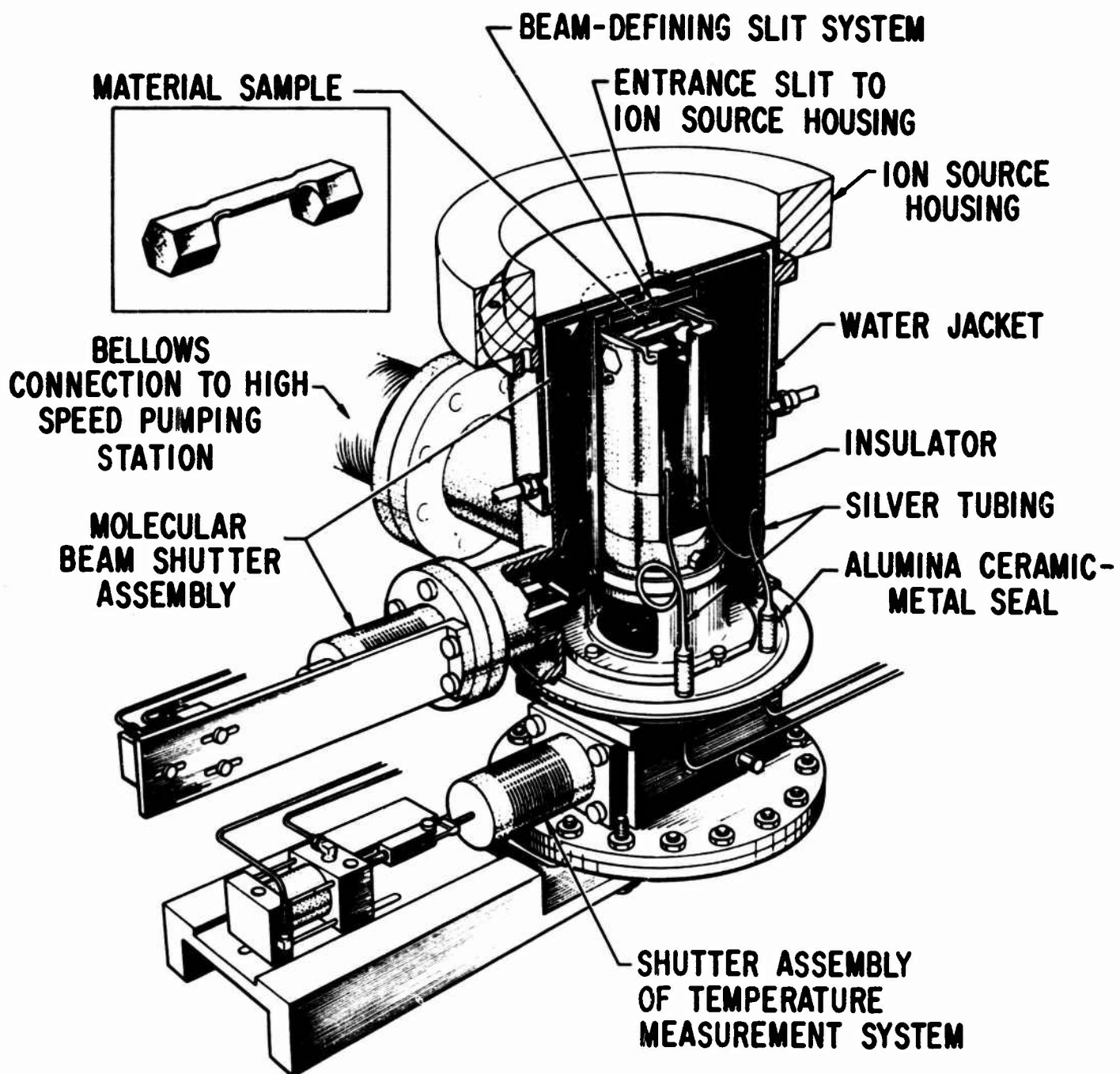


Figure 1. Cutaway View of Langmuir Cell and Water-Cooled Vacuum Housing

The specimen, mounted in a pair of water-cooled copper electrodes (Fig. 1), was resistively heated with alternating current supplied from a 7-kVA transformer. Power input data were obtained using automatic recording digital voltmeters that measured the voltages developed across the graphite specimen and across a $4\text{-m}\Omega$ standard resistor connected in series with the specimen. The carbon species evaporating from the graphite surface were collimated by the beam-defining slit system of the heat shield and the ion source. The slits of the heat shield were spatially oriented to the entrance slits of the ion source such that only those atoms and molecules that vaporized from the center portion of the heated specimen, a rectangular area approximately 4 mm long and 1.5 mm wide, were permitted to impinge upon the first slit of the ion source. The resulting beam passed not only through a system of beam-defining slits of the ion source but also through a pair of deflector plates that removed charged particles before the beam entered the ionizing region of the ion source where it was partially ionized by an electron beam of controlled energy. The ionization potentials of neon, xenon, and argon were used as reference voltages in adjusting the electron energy to 17 eV.

Surface temperature was measured using either a disappearing-filament optical pyrometer (PYRO Micro-Optical Pyrometer) or an automatic recording optical pyrometer (Leeds and Northrup, Model 8640) fitted with special optics to permit focusing on targets of 0.81-mm diam. The pyrometers were calibrated using a tungsten strip lamp calibrated by the National Bureau of Standards at brightness temperatures up to 2300°K ; above this temperature, the Molarc radiation source was used to check the pyrometers at 2800° , 3300° , and 3800°K using appropriate filters provided by the National Bureau of Standards. In addition, the performance of the automatic recording pyrometer was checked by measuring the temperature of incipient melting of molybdenum and tungsten strips in the Langmuir vaporization cell at low pressures. Using the spectral emissivity data reported by Allen, et al.,⁴

we observed the melting temperatures for molybdenum and tungsten to be 2906° and 3647°K , respectively; literature values for molybdenum and tungsten melting temperatures are 2895° and 3683°K , respectively.⁴

Each graphite specimen was of the form shown in the insert of Fig. 1 so that the temperature gradient from the center to either end of the specimen could be held to a minimum. The observed temperature gradient from the center in either direction within 2.5 mm from the center was found to be less than 10 deg. No apparent temperature gradient was observed across the 6.35-mm width of the specimen. Since the temperature of the back surface was monitored rather than that of the front surface, the difference between the two surface temperatures was determined using conventional and pyrolytic graphites and tungsten strips. The difference was found to be less than 10 deg, with the temperature of the front surface being higher. This discrepancy was attributed to the use of a single radiation shield on the back surface and three radiation shields on the front surface of the graphite specimen. Each brightness temperature reading was corrected for transmission and reflection losses from the Pyrex window, and for the emissivity of graphite. For the conventional graphites, emissivity corrections were calculated from emissivity data on machined-surface graphites reported by Grenis and Levitt.⁵ "Conventional graphites" will be used herein to describe molded and extruded graphites that are usually formed from petroleum-coke and coal-tar pitch binder. Insufficient data exist on the spectral emissivity of the C- and A-face of pyrolytic graphite. Herein, "C-face" refers to the "as-deposited" surface of the pyrolytic graphite specimen, and means that the crystallites are oriented such that their basal planes, or a,b-axes, are essentially parallel to the deposition plane. The A-face orientation of the specimen corresponds to the surface perpendicular to the "as-deposited" surface. Emissivity corrections for the C-face of pyrolytic graphite for brightness temperatures up to 2500°C were calculated from spectral emissivity data determined by Champetier.⁶ For brightness temperatures above 2500°C , a

constant emissivity value of 0.76 was assumed. This value was selected because a survey of the literature showed that most of the spectral emissivity data at the pyrometer wavelength ($\sim 0.65 \mu$) fell between 0.70 and 0.80 for both the C- and A-faces,⁶⁻¹¹ and that the temperature coefficient of spectral emissivity was nearly zero.¹⁰⁻¹¹ The same corrections were applied to the brightness temperature readings taken on the A-face.

Figure 2 is a photograph of the high-resolution, double-focusing mass spectrometer and the Langmuir vaporization cell, with its associated equipment.

B. GENERAL PROCEDURE FOR MASS SPECTROMETER ANALYSIS OF CARBON VAPOR

The following general procedure was used in studying the free vaporization of various grades of graphites. The electron energy of the electron beam was adjusted to 17 eV using the ionization potentials of neon, argon, and xenon as reference voltages. Each specimen was outgassed at 2100°K for 30 min, and at 2350°K for 1 hr. At each outgassing temperature, the gaseous products were analyzed mass spectrometrically. The major outgassing species were H₂, CO, CO₂, C₂H₂, and C₂H₄ for both types of graphite. During this outgassing procedure, which was continued until the CO⁺ ion intensity levelled off to the initial background intensity, the surface temperature was monitored using a disappearing-filament optical pyrometer. At the conclusion of this operation, the disappearing-filament pyrometer was replaced with the automatic recording optical pyrometer, which was focused at the center of the specimen and optically aligned to give the identical temperature reading as obtained with the disappearing-filament pyrometer.

Relative ion intensity measurements were made of the various carbon species vaporizing at a given surface temperature by magnetically scanning the entire mass range of interest at a scan rate of 40 sec per octave; appropriate corrections were made for mass discrimination effects. Relative ion intensity measurements were also verified by electrically scanning each mass separately. The temperature dependence of the ion intensity of each

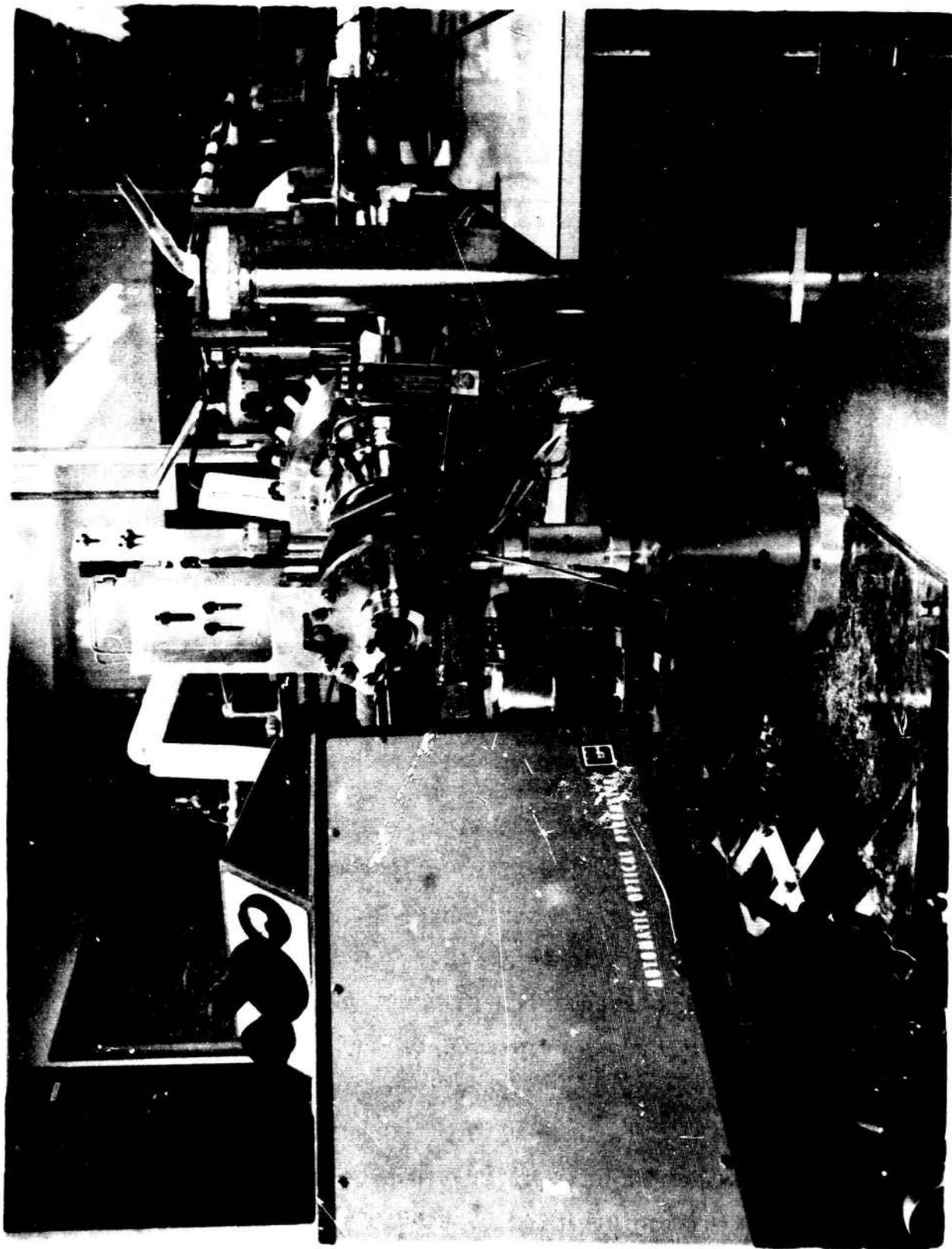


Figure 2. CEC Model 21-110 Mass Spectrometer and Langmuir Cell, with its Associated Equipment

species was determined by electrically scanning each mass separately at a scan rate of 80 ms per scan. In this latter mode of operation, the beam shutter and the shutter protecting the Pyrex window of the temperature measuring system were activated simultaneously; i.e., both shutters were opened simultaneously for approximately 5 sec. during which time temperature, ion current, and power input measurements were made. The background spectrum was continuously recorded during the time interval when both shutters were in the closed position; i.e., intercepting the molecular beam and the radiant energy.

C. MATERIALS

The graphite specimens were prepared, as shown in the insert of Fig. 1, from slabs of continuously nucleated pyrolytic graphite (High-Temperature Material Co.), ATJ and ZTA graphites (Carbon Products Division of Union Carbide Corp.), and from rods of UT-6 graphite (Ultra Carbon Corp.). Physical properties of these graphites are given in Table 1. All of the conventional graphite samples had machined surfaces. The pyrolytic graphite specimens were fabricated such that the original "as-deposited" C-face was retained; the edges were undercut 37 deg so that carbon vapor species vaporizing from these edges would not contribute significantly to the molecular beam. This undercutting is quite essential, especially for the pyrolytic graphite specimens, since the rate of vaporization from the A-face is greater than from the C-face.¹⁴

Table 1. Physical Properties of Graphites

Grade	Max Grain Size, mm	Bulk Density, g/cc ^a	C _o Spacing, Å ^b
ATJ	0.15	1.73	6.73
ZTA	0.15	1.95	6.72
UT-6	0.076	1.77	6.73
PG ^c	---	2.19	6.81

^aX-ray density = 2.266 g/cc (Ref. 12)

^bIdeal graphite C_o spacing = 6.708 Å (Ref. 13)

^cContinuously nucleated pyrolytic graphite

III. RESULTS AND DISCUSSION

A. PYROLYTIC GRAPHITE

Carbon species C_1 , C_2 , and C_3 were detected in the vapor above both the C- and A-face of pyrolytic graphite in the temperature range $2600^\circ - 3250^\circ K$. For the first time, C_4 and C_5 molecules were observed in the temperature range $2800^\circ - 3250^\circ K$; previously C_4 and C_5 molecules have been observed only in the vapor produced by impingement of a laser beam on pyrolytic graphite surfaces.¹⁵⁻¹⁸ The surface temperature produced by laser irradiation has been estimated to be approximately $4100^\circ K$;¹⁶ however, there is reason to believe that the conditions during evaporation by laser irradiation are significantly different from those during thermal evaporation.¹⁵ Polyatomic carbon molecules larger than C_5 were not detected even with the high-sensitivity photoplate detector. The absence of spectral lines on the photoplate corresponding to the high-molecular-weight carbon vapor species should not be construed as conclusive evidence for the absence of these species in the vapor because (1) the relatively short exposure times dictated by the lifetime of the sample may have precluded the detection of the parent-molecule ions of these species with the photoplate, and (2) the parent-molecule ions may have undergone metastable transitions prior to their arrival at the detector. Metastable transitions of ions of high-molecular-weight carbon species resulting in the loss of carbon atoms in groups of 3, 5, 9, and 11 atoms have been reported by Dörnenburg and Hintenberger.¹⁹

The most significant evidence for large carbon molecules was obtained from a study of the ionization efficiency curve for the C_3^+ ion shown in Fig. 3. The change in slope above 17.5 eV suggests that part of the C_3^+ ions are fragment ions resulting from electron-impact fragmentation of larger molecules.²⁰ The small quantities of C_4^+ and C_5^+ suggest that the progenitors of C_3^+ fragments are carbon species larger than the C_5 molecule. High-molecular-weight carbon species of masses up to about C_{30} have been observed by Vastola¹⁸ when the basal-plane surface of pyrolytic graphite is irradiated with a laser beam.

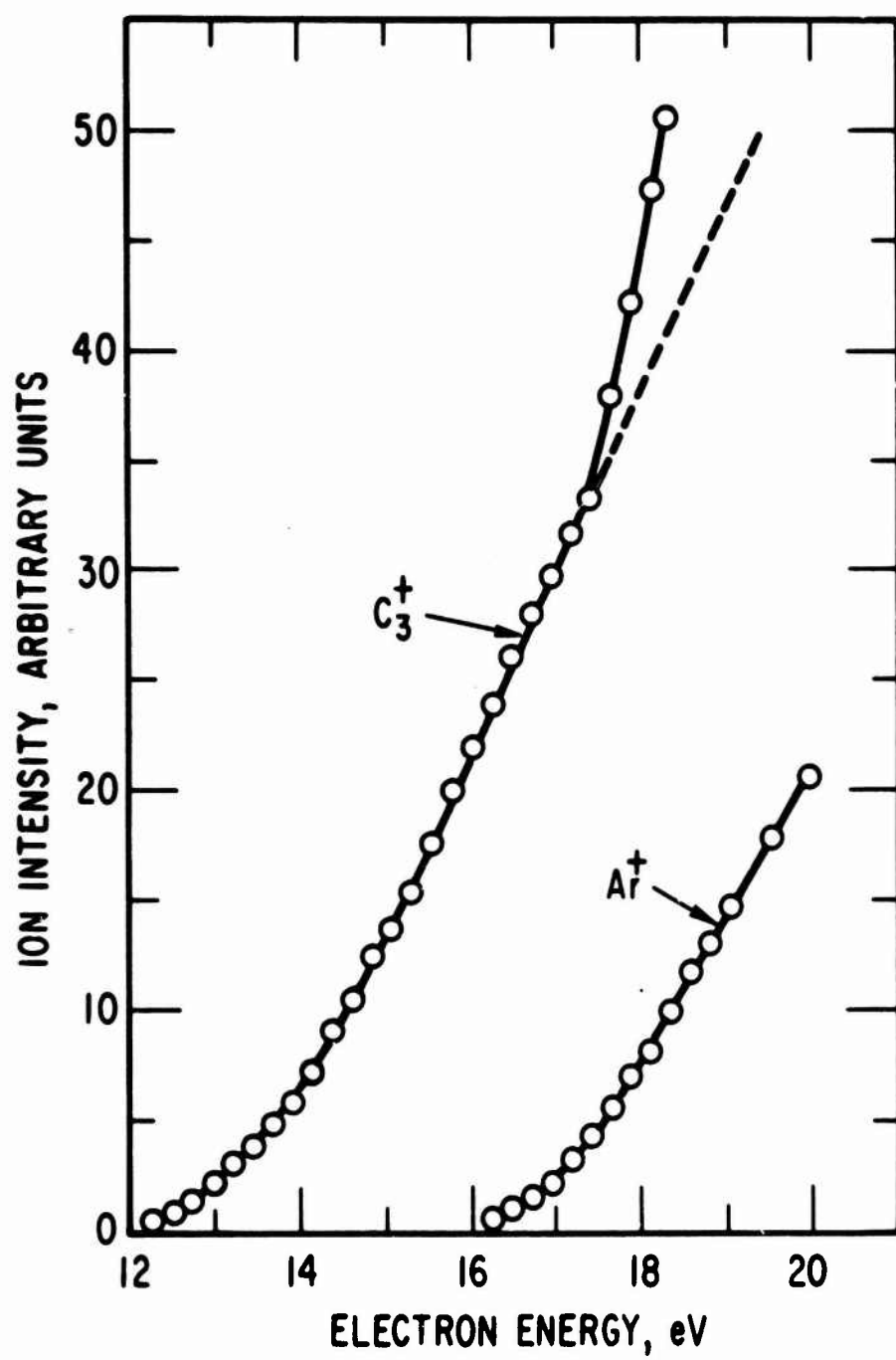


Figure 3. Ionization Efficiency Curve for C_3 Molecule from A-Face of Pyrolytic Graphite

Relative abundances of the carbon species were obtained from relative ion intensity measurements by assuming equal ionization cross sections, and are given in Table 2. The usual procedure of converting relative ion intensities into relative abundances by considering the relative ionization cross sections estimated from the additivity principle of atomic cross sections²¹ was not used because recent studies have indicated this principle does not always yield the correct electron-impact ionization cross sections.²²⁻²³ Below 3000°K, the relative abundances of C₁, C₂, and C₃ species for the "as-deposited" C-face vaporization agree with those reported by Burns, et al.,¹⁴ and show that the C₃ molecule is the most abundant species, contrary to the findings of Zavitsanos.²⁴ This difference in C₃ molecule abundance may have resulted from ion-molecule reactions in the ion source of our mass spectrometer and that used by Burns, et al. since the ions are accelerated in the same direction as the incident molecular beam. In the mass spectrometer used by Zavitsanos, ion-molecule reactions are not favored since the ions are accelerated in a direction orthogonal to that of the incident molecular beam. The relative abundance ratios for the A-face vaporization are significantly higher than for the C-face vaporization, and also differ from the values given by Burns, et al.¹⁴ The relative abundance ratio of C₁:C₂:C₃ for the A-face was found to be 1:2.4:5.9 at 2788°K, and not too different from that measured for equilibrium vaporization. The reported abundance ratio is 1:0.6:6 for equilibrium vaporization at 2755°K.²⁴ This disagreement in the distribution of species for the A-face may be indicative of an intrinsic difference in the distribution of species between continuously nucleated and surface-nucleated pyrolytic graphite.

It is not apparent from the published work of Burns, et al. which of the two types of pyrolytic graphite was examined. Evaporation studies on the A-face of surface-nucleated pyrolytic graphite are continuing in order to resolve this disagreement. The abundances of C₄ and C₅ molecules vaporizing from the C-face are identical, and the ratios C₃:C₄ and C₃:C₅ are

Table 2. Ion Intensity Ratios for Pyrolytic Graphite^a

Temperature, °K	Sample	C ₁ ⁺	:	C ₂ ⁺	:	C ₃ ⁺	:	C ₄ ⁺	:	C ₅ ⁺	Ref.
2500	A-face C-face	1	:	1.0	:	1.6	:	---	:	---	14
2740	C-face ^b	1	:	0.91	:	0.56	:	---	:	---	24
2740	C-face	1	:	0.93	:	1.5	:	---	:	---	This research
2940	C-face	1	:	1.6	:	2.6	:	0.024	:	0.024	This research
2788	A-face	1	:	2.4	:	5.9	:	---	:	---	This research

^aElectron energy: 17 eV.

^bElectron energy: 20 eV, surface nucleated pyrolytic graphite.

150:1 in the temperature range 2850° to 3260°K. Although accurate relative abundance measurements were not made for C₄ and C₅ species vaporizing from the A-face, preliminary data indicate that the abundances of these species are at least two orders of magnitude less than the C₃ molecule in the same temperature range.

The apparent activation energies of vaporization ΔE_a of C₁, C₂, C₃, C₄, and C₅ species were determined from the temperature dependence of the ion intensities in the temperature interval from 2600° to 3260°K. Since the rate of vaporization of a given species C_n from a surface is proportional to $I_{C_n} T^{1/2}$, where I_{C_n} is the ion intensity of the carbon species of interest and T is the surface temperature,²⁵ Arrhenius plots were made for each of the species by plotting $\log [I_{C_n} T^{1/2}]$ versus reciprocal temperature. Typical examples are presented in Fig. 4; these plots show no evidence indicating a change in vaporization mechanism over the temperature range studied. It should be emphasized that accurate relative ion intensities can not be deduced from these plots because measurements were not made under identical experimental conditions.

The apparent activation energies of vaporization for the carbon species were calculated from the slopes by least-squares analysis, and are given in Table 3. The apparent activation energies of vaporization of C₁, C₂, and C₃ from the C-face are 175, 193, and 201 kcal/mole, respectively, and are in agreement with the values reported by Zavitsanos.²⁴ Apparent activation energies of vaporization for C₄ and C₅ for C-face vaporization were measured for the first time and found to be 208 and 199 kcal/mole, respectively. The apparent activation energies of vaporization for C₃ and C₅ molecules from the A-face were found to be 197 and 201 kcal/mole, respectively, and equal to that from the C-face within the experimental error. These results suggest that the vaporization mechanism for these two species are similar for the two surfaces. For the C-face, the C₃ and C₅ molecules appear to evaporate predominantly from the edges of the a,b-plane (basal plane) of the crystallites at the grain boundaries and other

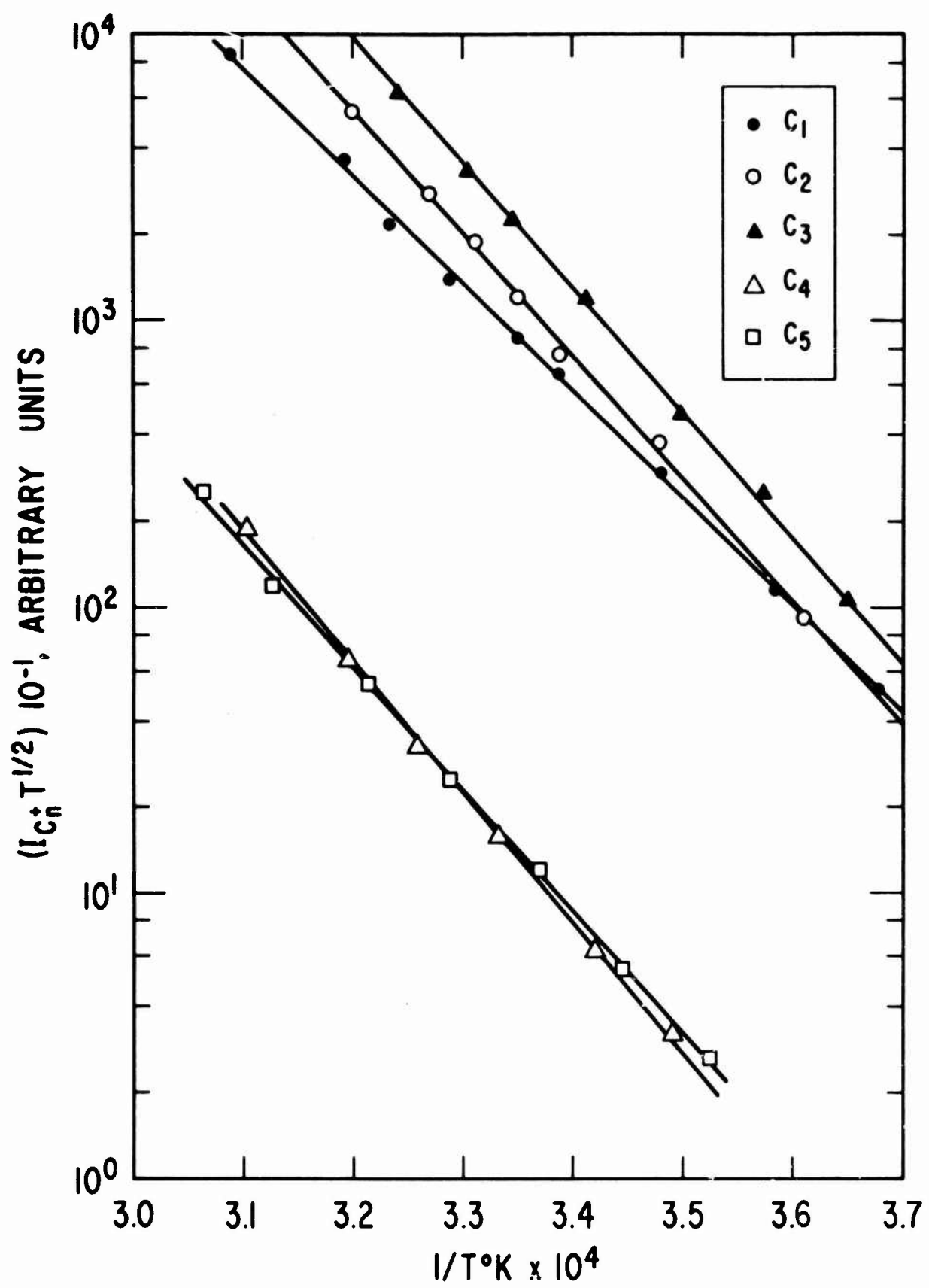


Figure 4. Arrhenius Plots for Carbon Species Vaporizing from C-Face of Pyrolytic Graphite

Table 3. Apparent Activation Energies of Vaporization of Carbon Species for Pyrolytic Graphite

Carbon Species	E_a , kcal mole ⁻¹	Temperature Range, °K	Ref.	Face
C ₁	180	2618 - 2760	24	C-face
C ₁	175±4	2664 - 3236	This research	C-face
C ₂	200	2618 - 2760	24	C-face
C ₂	193±5	2597 - 3226	This research	C-face
C ₃	207	2618 - 2760	24	C-face
C ₃	201±9	2597 - 3226	This research	C-face
C ₃	197±10	2638 - 2965	This research	A-face
C ₄	208±7	2864 - 3268	This research	C-face
C ₅	199±7	2837 - 3264	This research	C-face
C ₅	201±10	2890 - 3250	This research	A-face

discontinuities. Recently, etch pits have been observed with the scanning electron microscope on the C-face of pyrolytic graphite that had been heated to 3000°K.²⁶ These etch pits are believed to result from preferential evaporation of carbon at the sites of surface defects. Activation energies of vaporization for C₁, C₂, and C₄ from the A-face of continuously nucleated pyrolytic graphite have not yet been determined.

B. CONVENTIONAL GRAPHITES

The carbon vapor species observed in the vapor above pyrolytic graphite were also identified above conventional graphites. In addition, C₆ and C₇ molecules were observed at temperatures above 3000°K, but in very small quantities. The abundances of C₆ and C₇ molecules appear to be at least three orders of magnitude less than for the C₃ molecule. As in the case of pyrolytic graphite, no evidence has been obtained with the photoplate detector for higher-molecular-weight carbon species observed during evaporation under extreme conditions in high-frequency discharges,^{19,27-30} in vacuum spark,³¹⁻³² or in laser irradiation,¹⁵⁻¹⁶ apparently for the same reasons given earlier.

Significant differences in the relative abundances of the various carbon vapor species were found between the two types of graphites (Table 4). The abundance ratios were found to change erratically with temperature, and to exceed the ratio obtained under equilibrium vaporization condition. The reported relative abundance ratio for C₁:C₂:C₃ is 1:0.56:6.1 at 2500°K for equilibrium vaporization.³⁷ However, the most interesting difference was found in the time dependency of the species distribution at constant surface temperature. The relative ion intensities for C₁⁺, C₂⁺, and C₃⁺ varied with time at a given surface temperature, as shown in Table 5, whereas no variation in the relative ion intensities were observed with pyrolytic graphite for either the C-face or A-face vaporization. The initial ratio of 1:0.61:1.6 measured at 2627°K is in fair agreement with the value of 1:0.5:1.6 determined by Chupka and Inghram³⁴⁻³⁵ at 2450°K. This relative

Table 4. Ion Intensity Ratios for Conventional Graphites^a

Temperature, °K	Sample	C ₁ ⁺	:	C ₂ ⁺	:	C ₃ ⁺	:	C ₄ ⁺	:	C ₅ ⁺	Ref.
2400	Spec ^b	1	:	---	:	6.7	:	---	:	---	33
2450	Spec	1	:	0.5	:	1.6	:	---	:	---	34,35
2700	Spec	1	:	---	:	---	:	0.02	:	0.1	35,36
2318	UT-6	1	:	1.7	:	17	:	---	:	---	This research
2690	ATJ	1	:	0.45	:	6.3	:	---	:	---	This research
2715	ATJ	1	:	1.6	:	23	:	---	:	---	This research
2730	UT-6	1	:	1.5	:	30	:	---	:	---	This research
2866	UT-6	1	:	1.9	:	20	:	0.11	:	0.18	This research

^aElectron energy: 17 eV.

^bSpectroscopic grade graphite.

Table 5. Variation in Ion Intensity Ratio with Time
at 2627°K for ZTA Graphite

Time, min	Ion Intensity Ratio			
	C_1^+	:	C_2^+	C_3^+
0	1	:	0.61	1.6
3	1	:	0.65	3.2
6	1	:	0.91	4.4
9	1	:	0.98	8.5
13	1	:	0.96	12
23	1	:	1.3	21
120	1	:	2	40

^a Approximate

ion intensity ratio changed continuously with elapsed heating time until a limiting value of approximately 1:2:40 was attained. Concomitant increases of roughly 2, 3, and 20 times the original were observed in the magnitude of the ion intensities for C_1^+ , C_2^+ , and C_3^+ , respectively. This behavior was observed in all the conventional graphites investigated, regardless of the grain sizes or initial orientation of the crystallites. This time dependency of species distribution may account for the wide difference in relative abundance ratios published in the literature. At temperatures below about 2900°K, small differences in the rate of attainment of the limiting value were observed between the various grades of conventional graphites; however, even these differences disappeared when the specimens were heated to temperatures above 2900°K. The question of whether the total mass-loss for the different grades of graphite is identical remains unanswered, since mass-loss measurements have not yet been made.

The increase in ion intensities and change in the distribution of carbon species observed during extended heating at 2627°K can be explained by the following plausible vaporization mechanisms. Conventional graphites, consisting of a crystalline phase and an amorphous carbon binder phase, are essentially porous solids; hence, the total effective vaporizing surface area is comprised of the machined-surface area and the surface areas of the internal volumes (closed and open pores, crevices, channels), which are highly tortuous in the bulk of the solid. When these graphites are resistively heated, temperature gradients may develop at crystal defects, at discontinuities at the grain and phase boundaries, and at the sites of the internal voids. Enhanced vaporization may occur at localized hot spots because of these temperature gradients, resulting in continuous exposure of new crystal faces with different vaporization and condensation coefficients for the various carbon species. These continuous changes in surface area and surface morphology may partly account for the increase in ion intensities and the gradual change in species distribution. The vaporization of atoms and molecules from the surfaces of the closed and open pores may also produce profound

effects on the magnitude of the ion intensities and on the distribution of species in the following manner: The pores with very small orifices could act as small effusion cells; hence, the partial pressures of carbon species within these pores would gradually reach steady-state values. Concomitantly, the composition of the effusing vapor would change continuously until steady-state conditions were attained. The steady-state pressures could or could not be equal to the equilibrium vapor pressures, since establishment of equilibrium condition would depend on the relative sizes of the orifices and the pores.³⁸ On the other hand, the partial pressures of the carbon species within the closed pores could reach equilibrium values before these pores opened. As vaporization proceeds, these closed pores would gradually open, with the subsequent release of carbon vapors into the low-pressure regions of the vacuum chamber and into the tortuous channels that connect these pores to the plane of the machined surface. Under these conditions, the resultant composition of the effusing vapor could be either frozen to the vapor within the closed pores due to sonic flow, or continuously changing through the formation of high-molecular-weight carbon species by condensation and polymerization processes³⁹ due to supersonic flow.

Since most of the pores are situated within the bulk of the specimen, the vapors escape into the highly tortuous channels whose cross-sectional dimensions are relatively small, compared to the mean free paths of the carbon vapor species. Consequently, the atoms and molecules may collide with the channel walls many times before escaping the solid. Since vapor-solid interactions are considered to involve adsorption, surface diffusion, and re-evaporation,⁴⁰⁻⁴¹ mass transport to the plane of the machined surface can occur not only by gas-phase effusion but also by diffusion of atoms and molecules in the adsorbed layer on the channel walls.⁴² Self-diffusion of carbon has been reported to be quite appreciable at these high temperatures.⁴³⁻⁴⁴ Under these conditions, the relative abundances of the carbon species that arrive at a surface where free-vaporization condition exists depend on (1) the number of times the atoms and molecules collide with the channel walls,

(2) surface morphology, and (3) the condensation and vaporization coefficients of the individual carbon species on the various crystal faces of the internal voids. Preferential condensation of C_1 and C_2 on the cooler surfaces near the exit end of the channels could occur because of temperature gradients along these tortuous channels, due to radiation cooling near the machined-surface, and because of the low condensation and vaporization coefficient of C_3 , as compared to C_1 and C_2 . The condensation coefficients for C_1 and C_3 on graphite at 2300°K are reported to be 0.4 and 0.1, respectively;⁴⁵ the vaporization coefficients for C_1 , C_2 , and C_3 at 2500°K are roughly 0.2, 0.4, and 0.04, respectively.^{14,24,46} In addition, diminution of C_1 and C_2 could occur due to gas-phase and surface-recombination reactions. In essence, the continuous transformation of closed pores to open pores, and vice versa, the gradual attainment of steady-state vapor pressures in the open pores, the continuous changes in surface areas and surface morphology, and the continuous diminution of C_1 and C_2 by preferential condensation and by recombination reactions could account for the relatively large abundance of C_3 and for the time dependency of species distribution at constant surface temperature.

Corroborating evidence for the preceding postulations were obtained from photomicrographs of the cross section of the heated specimen and from x-ray diffraction analysis of the heated graphite surfaces. In the photomicrographs shown in Fig. 5 the redeposited carbon has an appearance similar to that of the C-face of pyrolytic graphite. These photomicrographs show the presence of carbon deposits near the outer surfaces, but give no evidence of redeposited carbon in the center section of the specimen. X-ray diffraction data on the powdered sample of the surface yielded two interlayer distances, $C_o = 6.712\text{\AA}$ and $C_o = 6.842\text{\AA}$. The latter C_o spacing is indicative of a highly turbostratic graphite¹³ and evidently corresponds to the redeposited carbon. The C_o spacing of the center portion was found to be 6.712\AA — a value 0.010\AA lower than that for the unheated specimen, indicating that some graphitization had occurred during vaporization.⁴⁷ Identical results

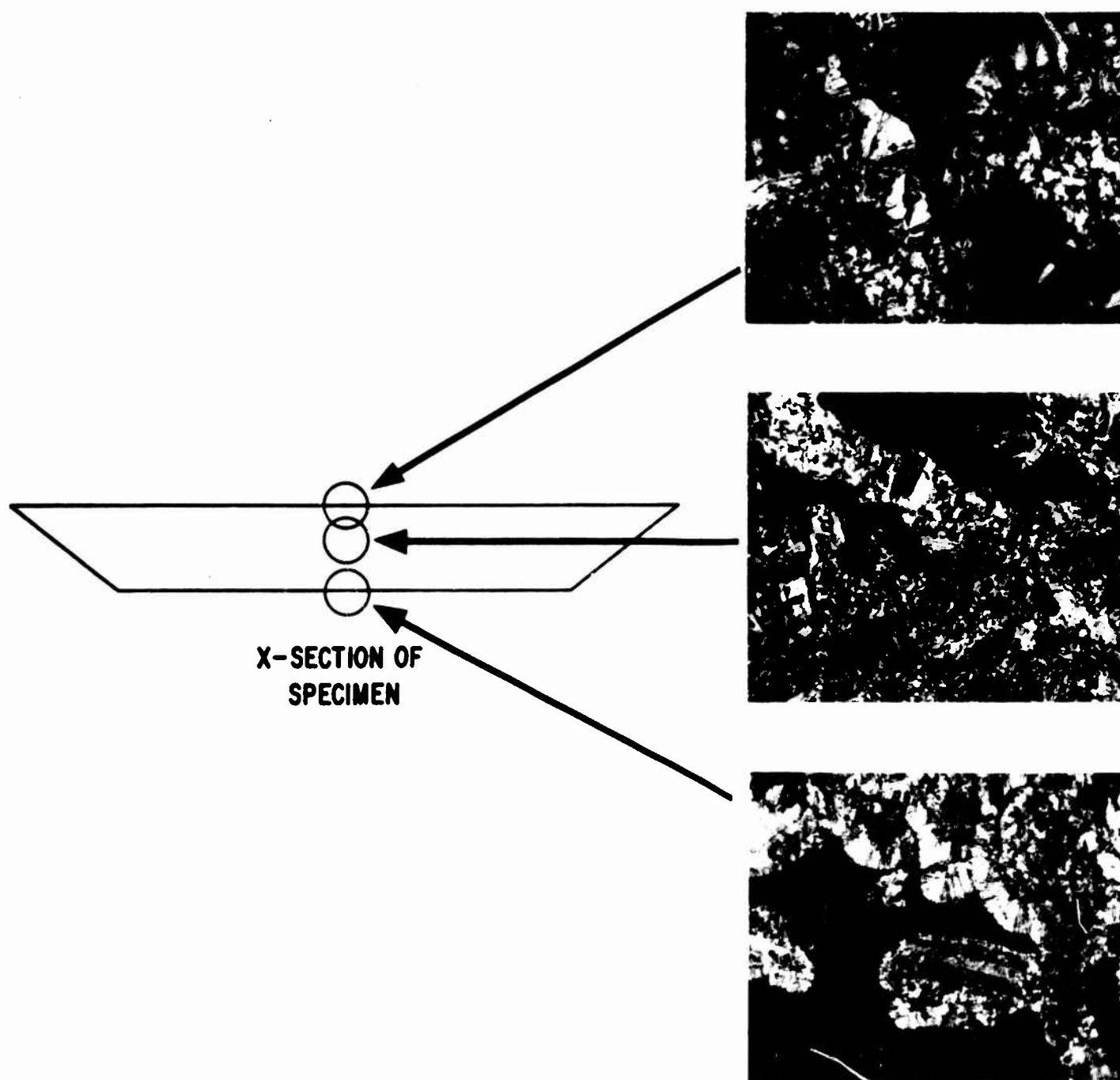


Figure 5. Photomicrographs of Cross Section of ZTA Graphite Heated to 2627°K

were obtained from a specimen heated under conditions where the carburized tantalum heat shields were removed and the carbon vapors were allowed to strike the walls of the water-cooled vacuum housing located 2.54 cm from the sample surface. These results suggest that the redeposited carbon does not result from condensation of carbon species reflected from the surrounding heat shields.

To minimize the effects of the time rate of change of carbon species on the determination of activation energies of vaporization, measurements were made as rapidly as possible of the temperature dependence of the ion intensities. The time required to obtain the necessary data at each temperature was less than 10 sec. Arrhenius plots of the apparent rates of vaporization of carbon species for UT-6 graphite are shown in Fig. 6. The rates of vaporization of the carbon species increased rather suddenly at temperatures above about 2900°K, indicating a possible change in evaporation mechanism. Similar vaporization behavior was observed with ATJ and ZTA graphites at temperatures above about 3000°K (Fig. 7). This large increase in the vaporization rates did not appear to be the result of errors in temperature measurements. Plots of surface temperature versus power input for the C₃ vaporization data for ATJ and ZTA graphites are shown in Fig. 8. These plots indicate that the errors in temperature measurements above 3000°K were too small to account for the large increase in the vaporization rate of the C₃ molecule. The abrupt increase in the rates of vaporization appears to reflect a genuine change in the overall vaporization process, since no similar changes in the vaporization rates were observed for either the C-face or the A-face of continuously nucleated pyrolytic graphite in the temperature range 2600° - 3260°K. This difference in vaporization behavior between conventional and pyrolytic graphite at temperatures above about 2900°K may be attributed to the vaporization of carbon from the binder phase; i.e., although evaporation of carbon from the crystalline phase and binder phase are occurring simultaneously, the vaporization of polyatomic carbon species from the binder phase is the predominant process above this temperature. As yet, no definitive

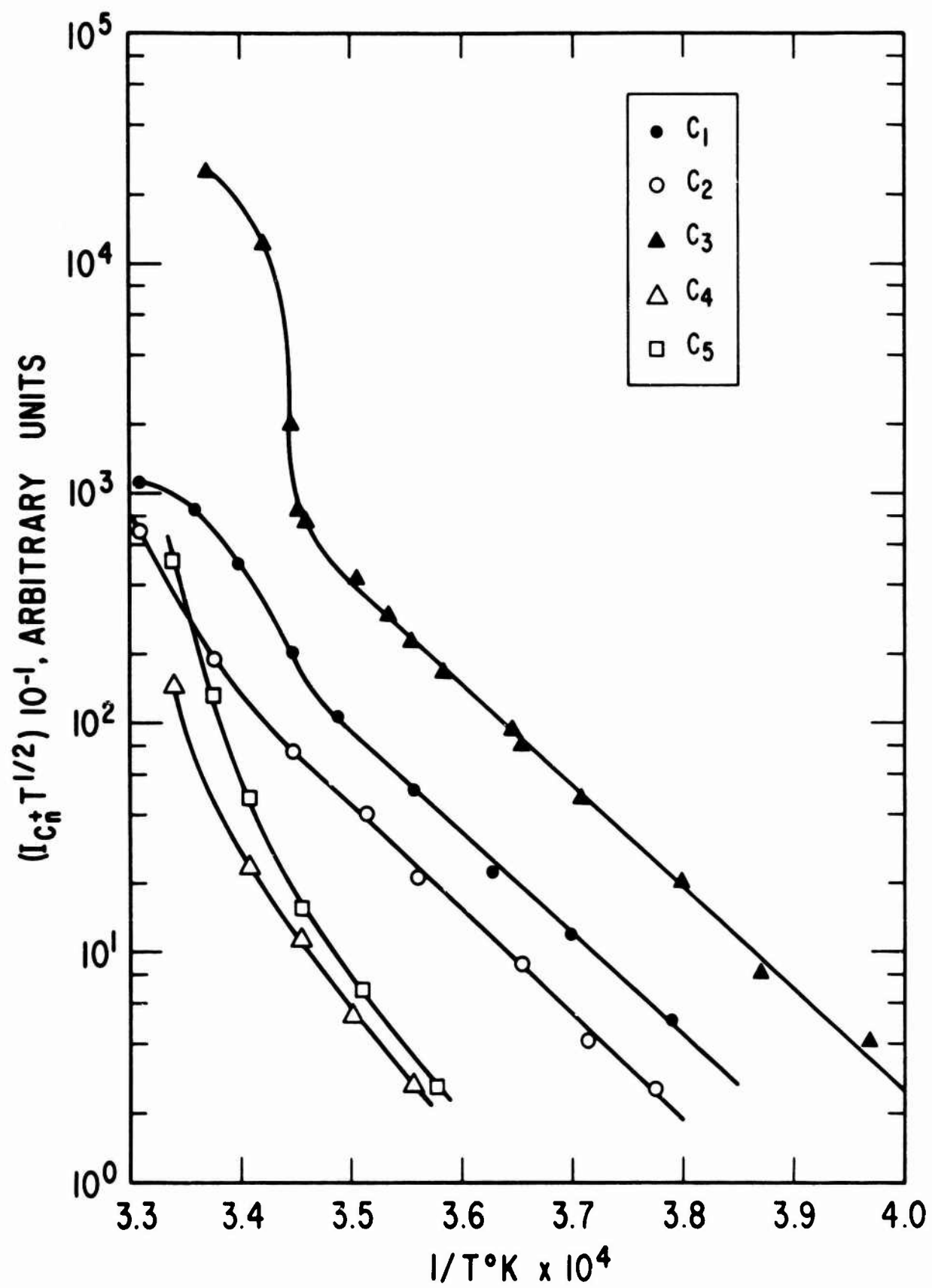


Figure 6. Arrhenius Plots for Carbon Species Vaporizing from Machined Surfaces of UT-6 Graphite

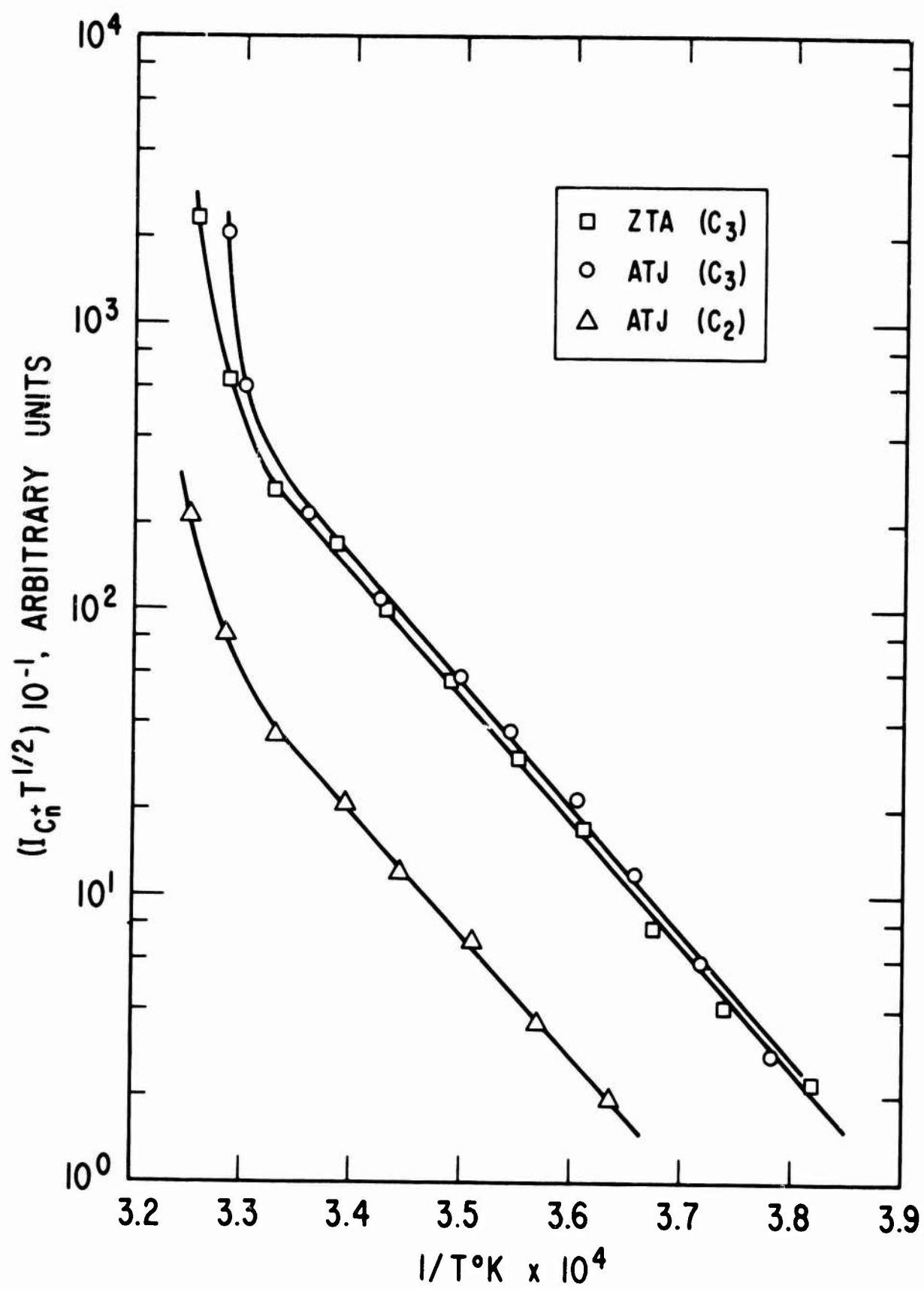


Figure 7. Arrhenius Plots for C₂ and C₃ Molecules Vaporizing from Machined Surfaces of ATJ and ZTA Graphites

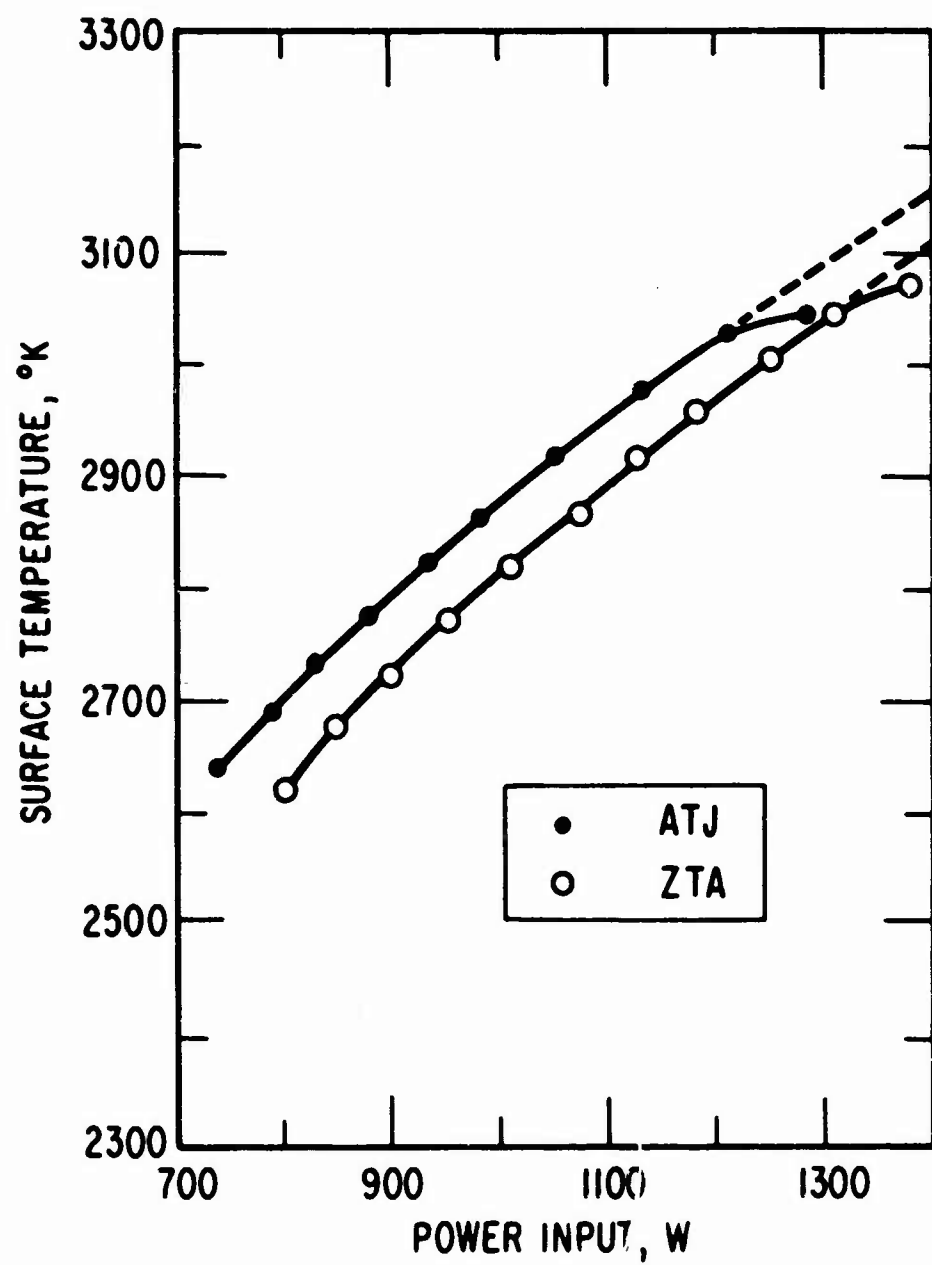


Figure 8. Variation of Surface Temperature with Power Input for ATJ and ZTA Graphites

experiments have been carried out to confirm this hypothesis; nevertheless, other experimental observations lend credence to this proposed vaporization process.

The sudden increase in the rates of vaporization was accompanied by the gradual appearance of fine particles in the vapor. These incandescent particles were evidently crystallites leaving the surface after the surrounding amorphous carbon binder phase had essentially completely vaporized. As yet, the presence of particles in the vapor above either the C- or A-face of pyrolytic graphite has not been observed, even at 3250°K under free vaporization condition; hence, it is not believed that these particles result from condensation of high-molecular-weight carbon vapor species. These particles were clearly visible when the disappearing-filament optical pyrometer was used to measure the surface temperatures above 2950°K . Corroborating evidence for the presence of these particles was obtained using the automatic recording optical pyrometer. Above temperatures of about 2950°K the output of the pyrometer was observed to reach a maximum in about 1.5 sec after an increase in power input, remain constant for approximately 1.5 sec, and then gradually decrease. During the latter 3.5 sec of the 5-sec measurement cycle, the ion current of the carbon species of interest and the power input remained constant, and no carbon deposits were found on the Pyrex window. It is believed that the apparent decrease in the brightness temperature resulted from scattering of radiation by the particles. The relationship between the temperature at which these particles appear and graphitization temperature and/or grain size was not investigated. Other evidence supporting the hypothesis that the vaporization of carbon species from the amorphous carbon binder phase is the predominant process above 2900°K is seen in the levelling off of the rate of vaporization of the C_3 molecule (Fig. 6), and the decrease in the rate of vaporization of the C_5 molecule (Fig. 9). This levelling off and decrease in rates of vaporization could result from depletion of the amorphous carbon binder, and the onset of these changes should depend on the previous heating history of the specimen. It

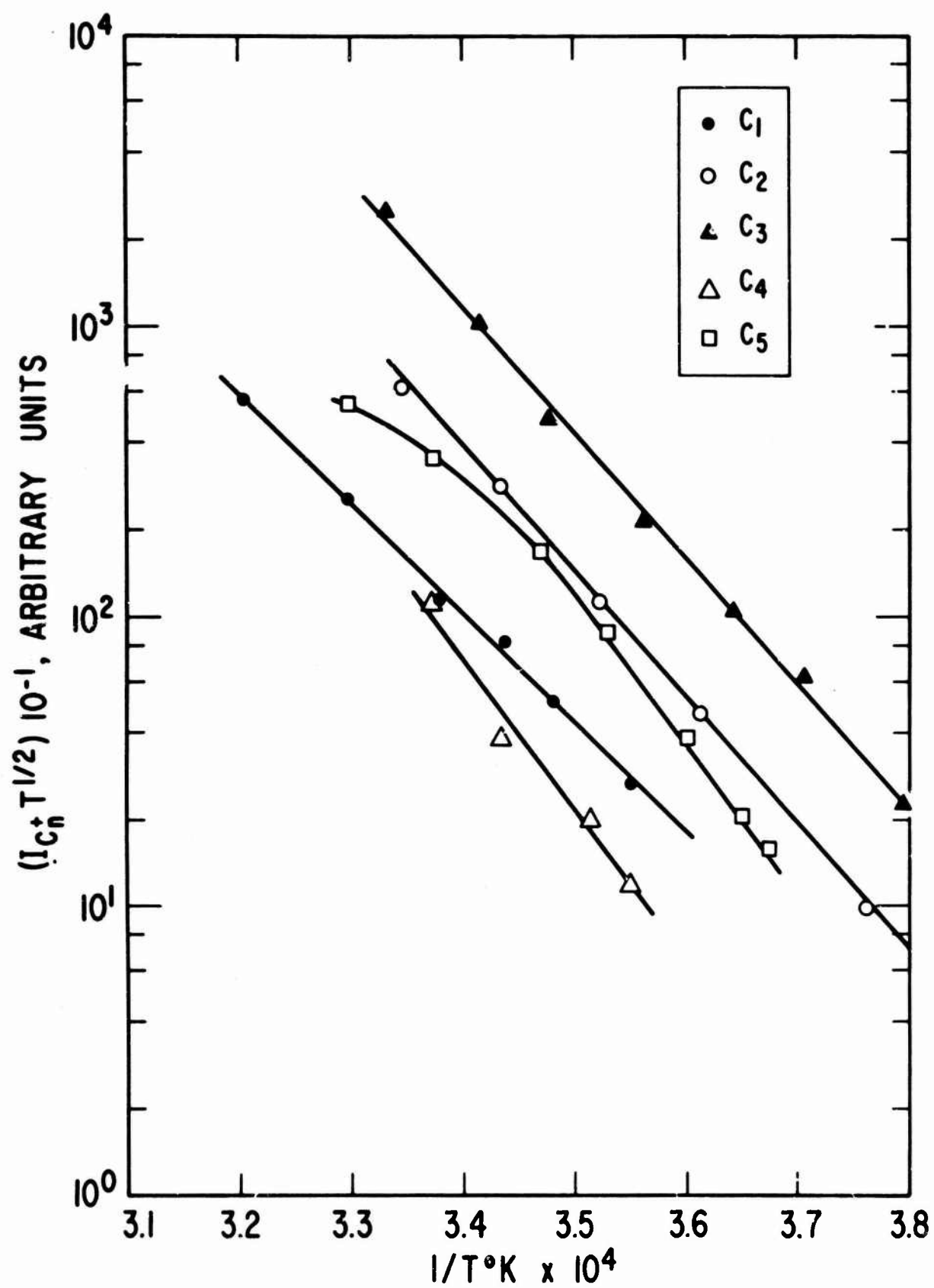


Figure 9. Arrhenius Plots for Carbon Species Vaporizing from Machined Surfaces of Conventional Graphites After Specimens Were Heated to 2950°K

was observed that if conventional graphites are subjected to prolonged heating to temperatures above 2900°K , the heated zones of the specimens not only flake off in chunks, but disintegrate into fine powdery material, determined by x-ray analysis to be graphite.

The preferential evaporation of carbon from the binder phase at these high temperatures is believed to be an intrinsic property of conventional graphites, and does not appear to be related to the method of heating. Recently, Whittaker²⁶ observed the ejection of particles at about $2900 \pm 50^{\circ}\text{K}$ when conventional graphites were heated by the radiative heating technique.

Apparent activation energies of vaporization for species C_2 and C_3 of ATJ graphite and C_3 of ZTA graphite were calculated from the linear portions of the Arrhenius plots shown in Fig. 7, and were found to be 194, 200, and 199 kcal/mole, respectively. These values are in excellent agreement with the activation energies of vaporization for C_2 ($\Delta E_a = 193$ kcal/mole) and for C_3 ($\Delta E_a = 201$ kcal/mole) obtained for pyrolytic graphite. These data suggest that, for conventional graphites, the vaporization of carbon from the crystalline phase is the predominant process up to the temperature at which a sudden increase in the rates of evaporation is observed. The excellent agreement in the activation energies of vaporization between the two types of graphite indicates that no serious errors were introduced into the measurements of the temperature dependence of the C_2^+ and C_3^+ ion intensities by the time rate of change of carbon species. The apparent activation energies of vaporization given in Table 6 were calculated from the linear portions of the Arrhenius plots, with exception of those for species C_4 and C_5 ; apparent activation energies of vaporization for these two species were obtained by first heating the specimens to 2950°K for about 5 sec, rapidly cooling to 2000°K , and subsequently measuring the temperature dependence of the ionic species of interest. Typical Arrhenius plots are shown in Fig. 9 for species C_4 and C_5 , as well as for other species. Preheating of the specimens enhanced the ion intensities of all the species and permitted us to measure the temperature dependency of ion intensities at lower temperatures. The increase in ion

Table 6. Apparent Activation Energies of Vaporization of Carbon Species from Machined Surfaces of Conventional Graphites

Carbon Species	E_a , kcal mole ⁻¹	Temperature Range, °K	Ref.
C ₁	179±10	T _{ave} = 2000	49
C ₁	177±6	T _{ave} = 2000	34
C ₁	178±10	T _{ave} = 2400	33
C ₁	179±5	2600 - 3000	This research
C ₂	199±20	T _{ave} = 2400	33
C ₂	200±10	T _{ave} = 2500	34
C ₂	195±5	2600 - 2950	This research
C ₃	178±10	T _{ave} = 2400	33
C ₃	200±10	T _{ave} = 2500	34
C ₃	197±10	2600 - 3000	This research
C ₄	241±10	2800 - 2950	This research
C ₅	242±6	2700 - 2950	This research

intensities may have resulted from the increase in surface area and from the conversion of closed pores to open pores. Apparent activation energies of vaporization obtained by this technique for species C_1 , C_2 , and C_3 were found to be in excellent agreement with those calculated from the linear portions of the Arrhenius plots for specimens that had not been previously heated to 2950°K . The apparent activation energies of evaporation for species C_4 and C_5 were found to be 241 and 242 kcal/mole, respectively — roughly 40 kcal/mole higher than the corresponding activation energies of vaporization obtained for the C_4 and C_5 species of pyrolytic graphite. This difference in activation energies of vaporization could have resulted from the porosity of the conventional graphites. In heat-treated specimens, it is possible that most of the closed pores have been opened, and that a large portion of the carbon vapor emanates from these small effusion cells. If this is the case, the apparent activation energies of evaporation should be comparable to the heats of vaporization. The reported heats of vaporization for C_4 and C_5 are 249 and 245 kcal/mole, respectively.⁴⁸ The difference in activation energies of vaporization could also have resulted from vaporization of carbon from the binder phase. If the vaporization of polyatomic carbon species from the amorphous carbon binder phase is the predominant process at these higher temperatures, then it is not unreasonable to expect the activation energies of vaporization for conventional graphites to be higher, since it is conceivable that it is more difficult to remove C_4 and C_5 molecules from a three-dimensional carbon lattice binder phase than from an essentially two-dimensional carbon lattice of pyrolytic graphite.

IV. CONCLUSIONS

Carbon species C_1 through C_5 are present in the vapor above both A- and C-face of continuously nucleated pyrolytic graphite in the temperature range $2600^\circ - 3250^\circ\text{K}$, with C_3 being the predominant species. Abundances of C_4 and C_5 appear to be at least two orders of magnitude less than that of C_3 . Identical activation energies of vaporization for carbon species vaporizing from the A- and C-face suggest that the vaporization mechanism is identical for the two surfaces. The vaporization of carbon species from the a,b-plane (basal plane) edges of the crystallites at the grain boundaries, other discontinuities, and surface defects appear to be the predominant process for C-face vaporization. There is no evidence of either a change in vaporization mechanism or anomalous changes in the distribution of species with time at constant surface temperature in the temperature range $2600^\circ - 3250^\circ\text{K}$ for continuously nucleated pyrolytic graphite.

The data presented herein for the free vaporization of conventional graphites suggest that at temperatures below about $2950 \pm 50^\circ\text{K}$, the vaporization of carbon species from the crystalline phase is the predominant process, and that at temperatures in excess of $2950 \pm 50^\circ\text{K}$, the vaporization of carbon species from the amorphous carbon binder phase is the predominant process. This abrupt transition in the relative importance of the two vaporization processes appears to produce profound effects on the vaporization behavior of conventional graphites at temperatures above $2950 \pm 50^\circ\text{K}$. The rates of evaporation of polyatomic carbon species increase abruptly, and the total mass-loss appears to occur by vaporization of carbon and ejection of crystallites. The preferential evaporation of carbon from the binder phase at these high temperatures appears to be an intrinsic property of conventional graphites, and does not appear to result from the method of heating. These anomalous vaporization phenomena demonstrate that extrapolation of low-temperature vaporization data to higher temperatures can not be made indiscriminately.

The observed time dependency of the relative abundances of carbon species at any given surface temperature below 2900°K appears to result from changes in surface area and surface morphology and the gradual transformation of closed pores to open pores. Plausible vaporization mechanisms are presented that account for the time dependency of species distribution at constant surface temperature for conventional graphites, and for the differences in activation energies of vaporization for C_4 and C_5 species for pyrolytic and conventional graphites. The effect of differential rates of vaporization on mass-loss under nonequilibrium conditions may now be the key to the understanding of some of the difficulties encountered when conventional graphites are used as thermal-protection materials in reentry vehicles.

REFERENCES

1. H. B. Palmer and M. Shelef, "Vaporization of Carbon," Chemistry and Physics of Carbon, P. L. Walker, Jr., Ed. (Marcel Dekker, Inc., New York, 1968), Vol. 4, p. 85.
2. M. Knudsen, Ann. Physik 28, 75, 999 (1909).
3. I. Langmuir, Phys. Rev. 2, 329 (1913).
4. R. D. Allen, L. F. Glasier, Jr., and P. L. Jordan, J. Appl. Phys. 31, 1382 (1960).
5. A. F. Grenis and A. P. Levitt, in Proceedings of the Fifth Conference on Carbon, (MacMillan and Company, New York, 1961), Vol. 2, p. 639.
6. R. J. Champetier, "Basal Plane Emittance of Pyrolytic Graphite at Elevated Temperatures," TR-0158(3250-20)-10, The Aerospace Corporation, El Segundo, Calif. (July 1967).
7. G. W. Autio and E. Scala, Carbon 4, 13 (1966).
8. G. M. Kibler, T. F. Lyon, M. J. Linevsky, and V. J. DeSantis, "Refractory Materials Research," WADD-TP-60-646, Part IV, General Electric Co., Evendale, Ohio (August 1964).
9. Marple, General Electric Research Laboratory, Schenectady, New York, (March 1963); results given in General Electric Pyrolytic Graphite Engineering Handbook, Optical Properties (May 1964).
10. J. D. Plunkett and W. D. Kingery, in Proceedings of the Fourth Conference on Carbon (Pergamon Press, New York, 1960), p. 457.
11. H. Y. Yamada, "A High-Temperature Blackbody Radiation Source--Supplement I: Spectral Emissivity of Graphite," BAMIRAC Report No. 4613-131-T, University of Michigan, Ann Arbor, Michigan (August 1966).

12. R. E. Nightingale, Nuclear Graphite (Academic Press, Inc., New York (1962), p. 89.
13. R. E. Franklin, Acta Cryst. 4, 253 (1951).
14. R. P. Burns, A. J. Jason, and M. G. Inghram, J. Chem. Phys. 40, 1161 (1964).
15. J. Berkowitz and W. A. Chupka, J. Chem. Phys. 40, 2735 (1964).
16. P. D. Zavitsanos, Carbon 6, 731 (1968).
17. F. A. Wodley and K. A. Lincoln, "Optical Observables in Re-entry Vehicle Wakes. Simulation and Chemistry," NRDL-TR-68-90, Naval Radiological Defense Laboratory, San Francisco, California (7 August 1968).
18. F. J. Vastola, Pennsylvania State Univ., University Park, Pennsylvania, preliminary results published in Chemistry and Physics of Carbon, P. L. Walker, Jr., Ed. (Marcel Dekker, Inc., New York, 1968), Vol. 4, p. 129.
19. E. Dörnenburg and H. Hintenberger, Z. Naturforsch., 14a, 765 (1959).
20. R. T. Grimley, "Mass Spectrometry," The Characterization of High-Temperature Vapors, J. L. Margrave, Ed. (John Wiley & Sons, Inc., New York, 1967), p. 195.
21. J. W. Otvos and D. P. Stevenson, J. Am. Chem. Soc. 78, 546 (1956).
22. J. Drowart, "Mass Spectrometric Studies of Vaporization of Inorganic Substances at High Temperatures," Condensation and Evaporation of Solids, E. Rutner, P. Goldfinger, and J. P. Hirth, Eds. (Gordon and Breach Science Publications, Inc., New York, 1964), p. 255.
23. J. H. Norman, "Vapor Pressures and Electron Impact Ionization Cross Sections," presented at the Fourth Western Regional Meeting of the American Chemical Society for Applied Spectroscopy, San Francisco, California, November 6-8, 1968.

24. P. D. Zavitsanos, "The Vaporization of Pyrolytic Graphite," Report No. R66SD31, Space Sciences Laboratory, Missile and Space Division, General Electric Company, King of Prussia, Pennsylvania (May 1966).
25. B. McCarroll, J. Chem. Phys. 46, 863 (1967).
26. A. G. Whittaker, The Aerospace Corporation, El Segundo, California (Private Communication).
27. H. Hintenberger, J. Franzen, and K. D. Schuy, Z. Naturforsch., 18a, 1236 (1963).
28. E. Dörnenburg, J. Hintenberger, and J. Franzen, Z. Naturforsch., 16a, 532 (1961).
29. N. Sasaki, M. Onchi, and J. Kai, Mass Spectry., (Tokyo), 12, 69 (March 1959).
30. W. M. Hickam and G. G. Sweeney, Rev. Sci. Instr., 34, 783 (1963).
31. W. L. Baun, F. N. Hodgson, and M. Desjardins, J. Chem. Phys., 38, 2787 (1963).
32. W. L. Baun and D. W. Fischer, J. Chem. Phys. 35, 1518 (1961).
33. R. E. Honig, J. Chem. Phys. 22, 126 (1954).
34. W. A. Chupka and M. G. Inghram, J. Chem. Phys. 21, 1313 (1953).
35. W. A. Chupka and M. G. Inghram, Met. Soc. Roy. Sci. Liege, 15, 373 (1955).
36. W. A. Chupka and M. G. Inghram, J. Chem. Phys. 22, 1472 (1954).
37. J. Drowart, R. P. Burns, G. DeMaria, and M. G. Inghram, J. Chem. Phys. 31, 1131 (1959).
38. G. M. Rosenblatt, J. Electrochem. Soc. 110, 563 (1963).

39. F. T. Greene and T. A. Milne, J. Chem. Phys. 39, 3150 (1963).
40. I. Langmuir, Phys. Rev. 8, 149 (1916).
41. M. Volmer and I. Estermann, Z. Physik 7, 13 (1921).
42. G. W. Sears, J. Chem. Phys. 22, 1252 (1954).
43. M. H. Feldman, W. V. Goettel, G. J. Dienes, and W. Gossen, J. Appl. Phys. 23, 1200 (1952).
44. F. J. Dienes, J. Appl. Phys. 23, 1194 (1952).
45. W. A. Chupka, J. Berkowitz, D. J. Meschi, and H. A. Tasman, Advances in Mass Spectrometry, R. M. Elliot, Ed. (Pergamon Press, New York, 1963), Vol. 2, p. 99.
46. R. J. Thorn and G. H. Winslow, J. Chem. Phys. 26, 186 (1957).
47. D. B. Fischbach, Nature 200, 1281 (1963).
48. T. A. Dolton, R. E. Maurer, and H. E. Goldstein, "Thermodynamic Performance of Carbon in Hyperthermal Environments," AIAA Paper No. 68-754, presented at the AIAA Third Thermophysics Conference, Los Angeles, California., June 24-26, 1968.
49. W. A. Chupka and M. G. Inghram, J. Chem. Phys. 21, 371 (1953).

UNCLASSIFIED

Security Classification

DOCUMENT CONTROL DATA - R&D		
(Security classification of title, body of abstract and indexing annotation must be entered when the overall report is classified)		
1. ORIGINATING ACTIVITY (Corporate author) The Aerospace Corporation El Segundo, California		2a. REPORT SECURITY CLASSIFICATION Unclassified
		2b. GROUP
3. REPORT TITLE High-Temperature Mass Spectrometry Volume I: Free Vaporization Studies of Graphites		
4. DESCRIPTIVE NOTES (Type of report and inclusive dates)		
5. AUTHOR(S) (Last name, first name, initial) Wachi, Francis M., and Gilmartin, Donald E.		
6. REPORT DATE 27 January 1969	7a. TOTAL NO. OF PAGES 46	7b. NO. OF REFS 49
8a. CONTRACT OR GRANT NO. F04701-68-C-0200	8a. ORIGINATOR'S REPORT NUMBER(S) TR-0200(4250-40)-6, Vol I	
b. PROJECT NO.		
c.	8b. OTHER REPORT NO(S) (Any other numbers that may be assigned this report) SAMSO-TR-69-124 VOL. I	
d.		
10. AVAILABILITY/LIMITATION NOTICES This document has been approved for public release and sale; its distribution is unlimited.		
11. SUPPLEMENTARY NOTES	12. SPONSORING MILITARY ACTIVITY Space and Missile Systems Organization Air Force Systems Command U. S. Air Force	
13. ABSTRACT Some of the differences in the published data on the free vaporization of conventional (ATJ, ZTA, UT-6) and pyrolytic graphites have been resolved. Relative abundances, relative rates of vaporization, and activation energies of vaporization have been measured for carbon species C ₁ through C ₅ , for conventional graphites in the temperature range 2800° - 3000°K, and for pyrolytic graphite in the temperature range 2600° - 3260°K. Differences in the free evaporation behavior of the two types of graphites are discussed. Plausible vaporization mechanisms are presented that account for the time dependency of species distribution at constant surface temperature for conventional graphites, and for the differences in activation energies of vaporization for C ₄ and C ₅ molecules vaporizing from pyrolytic and conventional graphites. The effects of the differential rates of carbon evaporation from the crystalline and binder phases on the free vaporization behavior of conventional graphites at temperatures greater than about 2950±50°K are described.		

DD FORM 1473
(FACSIMILE)

UNCLASSIFIED

Security Classification

UNCLASSIFIED

Security Classification

14

KEY WORDS

Pyrolytic graphite vaporization
Conventional graphite vaporization (ATJ, ZTA, UT-6)
Free evaporation
High temperature
Mass spectrometer
Species identification
Relative abundances
Relative vaporization rates
Vaporization mechanisms
Activation energies
Binder phase vaporization
Mass-loss carbon evaporation
Mass-loss particle ejection
Surface morphology
Surface defects
Crystallites

Abstract (Continued)

UNCLASSIFIED

Security Classification